

A COMBINED GNSS-DINSAR-IRT STUDY FOR THE CHARACTERIZATION OF A DEEP-SEATED GRAVITATIONAL SLOPE DEFORMATION

GIOVANNA PAPPALARDO^(*), SIMONE MINEO^(*), CHIARA CAPPADONIA^(**),
DIEGO DI MARTIRE^(***), DOMENICO CALCATERRA^(***), UMBERTO TAMMARO^(****),
EDOARDO ROTIGLIANO^(**) & VALERIO AGNESI^(**)

^(*)Università degli Studi di Catania - Dipartimento di Scienze Biologiche, Geologiche e Ambientali - Corso Italia, 57 - 95129 Catania (Italy)

^(**)Università degli Studi di Palermo - Dipartimento di Scienze della Terra e del Mare - Via Archirafi, 22 - 90123 Palermo (Italy)

^(***)Università degli Studi di Napoli Federico II - Dipartimento di Scienze della Terra, dell'Ambiente e delle Risorse - Via Cintia, 21
Complesso Universitario Monte Sant'Angelo - 80126 Napoli (Italy)

^(****)Istituto Nazionale di Geofisica e Vulcanologia, Osservatorio Vesuviano - Via Diocleziano, 238 - 80124 Napoli (Italy)

Corresponding author: chiara.cappadonia@unipa.it

EXTENDED ABSTRACT

La definizione dei modelli evolutivi e cinematici dei fenomeni di Deformazione Gravitativa Profonda di Versante (DGPV) è caratterizzata da un elevato grado di complessità a causa della loro notevole estensione ed articolazione in settori o unità tra loro disarticolate. D'altra parte, nonostante la loro bassa velocità di deformazione, a causa dell'accoppiamento morfodinamico con fenomeni franosi più superficiali e rapidi, nelle aree soggette a DGPV possono determinarsi condizioni di pericolosità geomorfologica elevate. Tra le evidenze morfologiche di tali fenomeni sono frequenti blocchi ruotati, scarpate, trincee, avvallamenti di cresta, fessure di trazione e/o rigonfiamenti vallivi o di piede.

Se il riconoscimento ed il rilevamento geomorfologico di tali fenomeni risulta complicato dal quadro estremamente variabile e composito di forme, ancora più complesso ne risulta il monitoraggio. Infatti, soprattutto in aree dove le DGPV sono particolarmente evolute, l'interpretazione del quadro deformativo osservato deve tenere conto del differente grado di radicamento (substrato o blocchi in deformazioni) dei vertici di monitoraggio, così come della variabilità plano-altimetrica e del range dinamico degli stessi spostamenti da misurare. Per tale motivo è importante integrare le metodologie tradizionali di rilevamento e analisi con ulteriori metodi di indagine forniti dal recente sviluppo scientifico-tecnologico, al fine di ottenere dati più affidabili e definire un modello di deformazione.

Nel presente lavoro vengono presentati e discussi i primi risultati di un'indagine integrata condotta sulla frana di Scopello, uno dei più rilevanti casi di Deformazioni Gravitative Profonde di Versante in Sicilia, dove la tettonica distensiva e compressiva hanno svincolato la porzione laterale di un complesso carbonatico fragile che poggia su un substrato marnoso-argilloso a comportamento duttile. Tale assetto è il risultato del sovrascorrimento delle successioni di piattaforma triassico-mesozoiche del dominio Panormide su quelle mioceniche del dominio trapanese. Lo spessore dello slab carbonatico varia da diverse centinaia di metri nel fianco sinistro, fino a poche decine di metri, lungo il fianco destro. Evidenze morfologiche del fenomeno in studio sono stati riconosciuti anche al di sotto del livello del mare, per una notevole estensione a largo della costa.

Lo studio delle principali caratteristiche strutturali che interessano gli ammassi rocciosi dell'area di Scopello è stato condotto mediante indagini geologiche e geomorfologiche sul campo, analisi aerofotogrammetriche, analisi dei modelli digitali del terreno (DTM) disponibili, rilievi di Termografia a Infrarossi, interferometria DInSAR ed acquisizione di misure GNSS. I rilievi di Termografia a Infrarossi, che permettono di definire le variazioni di temperatura superficiale rilevata in campo, sono stati condotti per analizzare le porzioni massive a contorno dell'area in frana e hanno consentito di rilevare una serie di sistemi di discontinuità associabili ai lineamenti tettonici generali dell'area. L'interferometria satellitare DInSAR è consistita nell'analisi di dati di archivio ottenuti dal processamento delle immagini ENVISAT acquisite per il periodo 2002-2010, dall'Agenzia Spaziale Europea nell'ambito del Piano Straordinario di Telerilevamento Ambientale (PST-A), sia in geometria ascendente che discendente; tali dati sono stati successivamente integrati con il processamento di immagini ad alta risoluzione Cosmo-SkyMed, dell'Agenzia Spaziale Italiana, per il periodo 2016-2018. L'analisi di dei dati per i due intervalli di tempo ha consentito di individuare settori di versanti caratterizzati da tassi di spostamento talvolta variabile, fino a 1.5 cm/anno, evidenziando, pertanto, differenti cinematismi. Infine, sulla base dei risultati di tre campagne di misure GNSS condotte su una rete di ventisette vertici distribuiti su tutta l'area in frana, è stato possibile riconoscere le deformazioni indotte da un evento pluviometrico intenso che, nel febbraio 2005, ha determinato l'attivazione di una serie di frane superficiali, con evidenti richiami sui corpi principali blocchi carbonatici sui quali è articolata ad oggi la DGPV di Scopello.

Sulla base dei risultati emersi, si dimostra come l'integrazione delle tre tecniche di indagine e monitoraggio consenta effettivamente di supportare l'interpretazione geomorfologica di un fenomeno di grande rilevanza scientifica, sia per la complessità del sistema, sia per il notevole grado di evoluzione raggiunto.

ABSTRACT

Large deep-seated gravitational slope deformation (DsGSD) are slope instability phenomena affecting high relief-energy hillslopes and characterized by a high degree of complexity, enhanced also by wideness of the affected area and lithological heterogeneity. A combined approach based on different remote survey methodologies is herein presented with the aim of characterizing one of the most relevant DsGSDs in Sicily (Italy). The Scopello landslide involves the external margin of an overthrust plane, where a rigid carbonate tectonic unit overlies a ductile clayey substratum. The evidence of structural discontinuities crossing the rock masses and of unstable rock mass portions were pointed out by IRT, whose results were combined with the analysis of morphological features retrieved from a DTM, highlighting the presence of regional systems controlling the rock fracturing. Three GNSS surveys have been carried out in 2004 and 2005 on a 27-vertex geodetic network, attesting up to 20cm deformations caused by the triggering of landslides in the substratum. DInSAR results, obtained from the processing and interpretation of ENVISAT and Cosmo-SkyMed images, both in ascending and descending geometry for the time span 2002-2018, allowed evaluating the displacement rates over the area, highlighting that the movement is still active in its upper sector.

KEYWORDS: Deep-seated Gravitational Slope Deformation, DInSAR, InfraRed Thermography, GNSS, Scopello landslide (Sicily)

INTRODUCTION

Deep-seated Gravitational Slope Deformations (DsGSDs) are counted among slow-evolution phenomena, affecting high relief-energy hillslopes and characterized by a size comparable to the whole slope against relatively small displacements (e.g. SORRISO-VALVO, 1984; SAVAGE & VARNES, 1987; VARNES *et alii*, 1989; DRAMIS & SORRISO-VALVO, 1994; CROSTA, 1996; PASUTO & SOLDATI, 1996; AGLIARDI *et alii*, 2001). However, despite their slow deformation rates, DsGSDs may either evolve into faster mass movements or trigger local landslide processes, thus gaining relevance even in terms of landslide hazard and risk. Among their typical morphological elements, double ridges, scarps, trenches, ridge depressions, tension cracks or toe bulges, can be counted, although their recognition is often sided by a certain degree of complexity according to the wideness of the area they are spread on.

This paper shows and discusses the results of the study of the Scopello DsGSD which was carried out by integrating InfraRed Thermography (IRT), Global Navigation Satellite System (GNSS), and Differential Interferometry SAR (DInSAR) surveys. In facts, as a direct consequence of the wideness and deepness of the involved rock volumes as well as of the very advanced stage of the Scopello landslide, the landscape is

characterized by a very rugged hummocky morphology, which makes as very hard to detect very small displacements in a so large areas at a time. Thus, integrated survey methodologies can be applied for the study of such a complex phenomenon, in order to achieve reliable-integrated data and to set up an evolutive model.

The study of the main structural features affecting the rock masses was carried out herein by field geomorphological surveys and Digital Terrain Model (DTM) analysis, coupled with IRT surveys. The latter is a scientifically recent application in the study of landslides, which proved a reliable tool for the characterization of rock masses, with specific reference to fracturing characterization and reconstruction of kinematic models, and complex landslides even in combination with other remote or indirect surveying methodologies (e.g. CASAGLI *et alii*, 2017; FIORUCCI *et alii*, 2018; PAPPALARDO *et alii*, 2018; PAPPALARDO & MINEO, 2019; PAPPALARDO *et alii*, 2020; DEVOTO *et alii*, 2020; FRODELLA *et alii*, 2021; PAPPALARDO *et alii*, 2021). At the same time, the displacement field for some studied time windows was reconstructed by integrating GNSS and DInSAR, with field surveys carried out in the time interval 2000, 2005 and 2006, for GNSS, 2002-2010 and 2016-2018, for DInSAR.

STUDY SITE

“Scopello landslide” actually refers to a near 5 km² large area, marked by a number of coupled complex/composite surface to deep-seated slope deformations, located at the south-eastern limit of the San Vito peninsula, along the north-western coast of Sicily (Fig. 1). The whole area includes a less than 1km wide morphologically depressed sector, gently sloping seaward for 3km in SW-NE direction, from the saddle of “Portella di

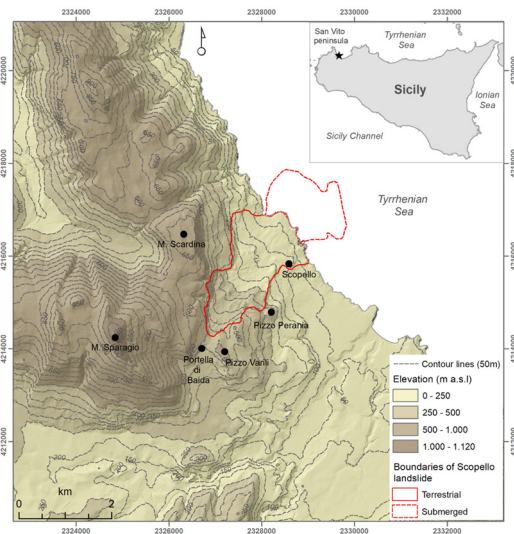


Fig. 1 - Geographic framing and hill-shaded representation of the study area

Baida” down to the seacoast, and the adjacent slope margins or whole reliefs of the set of surrounding hilly-mountainous areas. The central lower sector is characterized by an irregular or hummocky morphological features and is marked by a step along the longitudinal profile marking separating the narrow head sector from the lower two kilometers wide coastal zone. The hilly belt in the left flank is marked by steep scarps connecting the western foot-slopes of “Monte Scardina” (680 m a.s.l.) and “Monte Sparagio” (1110 m a.s.l.) to the central lower sector, whilst the right flank, with the exception of “Pizzo Varili” (511 m a.s.l.) an “Pizzo Perania” (331 m a.s.l.) in the upper hill sector, rather corresponds to highly disrupted blocks, more and more dispersed going toward the sea, where small stacks can be also recognized. The Scopello landslide includes also a very wide offshore sector (for about 1400 m far from the coast), as suggested by the isobaths pattern and confirmed by geophysical surveys (AGNESI *et alii*, 2006; SULLI *et alii*, 2021), corresponding to a long foot sector with a large number of dispersed blocks.

The geological setting of the area (Fig. 2) is marked (CATALANO *et alii*, 2011) by the superimposition of a more/less regular and thick slab, made of Triassic to Mesozoic platform carbonatic rocks, which overlies a ductile clayey/sandy marly substratum. This setting is the results of the continental collision since Middle Miocene (CATALANO *et alii*, 2013) that caused in this area the overthrusting of a Panormide platform domain derived unit on the Miocenic top formation of the Trapanese domain sequence. The thickness of the carbonatic slab ranges from several hundreds of meters in the left flank, down to one-hundred or few tens of meters, along the right flank.

Together with the Mio-Pliocenic overthrust limit, associated inverse high angle faults and subsequent Pleistocenic NW-SE/NE-SW normal faults segmented the whole slab/substratum stack. In particular, the whole right flank of the area corresponds to the more advanced thinned front of the overthrust structural unit of “Monte Sparagio”, which actually represents a ramp anticline. Besides, the head “V”-shaped sector is interrupted by a direct fault which lowers the whole coastal sector.

According to previous studies (AGNESI *et alii*, 1987, 2006, 2015, 2017; DI MAGGIO *et alii*, 2014), in light of its geologic setting and tectonic evolution, the mosaic of landforms in the Scopello area can be interpreted as mainly controlled by the activity of deep seated gravitational slope deformation phenomena triggered by the pleistocenic seaward lateral extensional unlocking of the stack of tectonic units; in facts the collapsing of the offshore sector concentrated in this marginal area high energy relief conditions, unlocking the overthrusting plane which was exposed to erosion (DI MAGGIO *et alii*, 2017).

Referring to the margin of the carbonatic slab, the following deformation phenomena are recognized (Fig. 3): in the left flank,

where the thickness of the slab is more than one-hundred meters thick, a great lateral spread to sagging phenomenon is active; in the right flank, where the thickness of the slab vanishes to some tens of meters, a number of lateral spreads, block differential settling, slides and tilting phenomena dismantle the slab into disarticulated smaller units. Probably due to a fault plane which runs along the longitudinal axis of the area, in the central lower sector, the dismantling of the rigid slab has been more intense

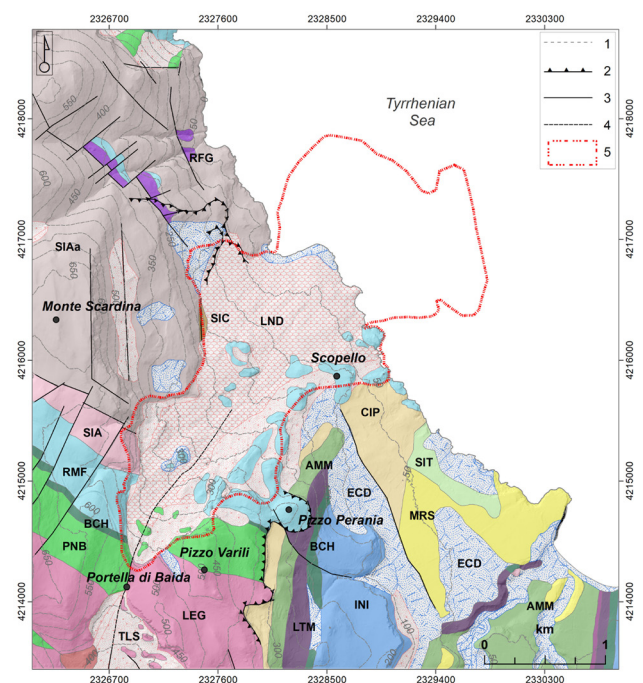


Fig. 2 - Geological setting of the area modified from CATALANO *et alii* (2011). LEGEND: 1 - Contour lines (50 m); 2 - Thrust; 3 - Normal fault; 4 - Strike-slip fault (uncertain); 5 - Terrestrial and submerged boundaries of Scopello landslide; TLS - Landslide deposits; ECD - Eluvial and colluvial deposits; SIT - Conglomerates, arenites, poor sorted coarse sands, bioclastic limestones; MRS - Cross-stratified calcarenites, calcirudites and conglomerates; CIP - Clays and sandy marls; RFG - Clays, sandy clays and quartz and glauconite-rich brown; LEG - Biocalcarenes and biocalcirudites; PNB - Calcarenites alternating with stratified calcirudites and carbonatic breccias; RMF - Limestones, dolomitic limestones and loferitic dolomites, loferitic breccias; SIA - Dololutes and doloarenites; SIAa - Carbonatic dolomites and dolomitic limestones; AMM - Marly calcilutites with intercalations of thin layers of marls and calcarenites; LTM - Marly limestones, laminated calcilutites with chert; BCH - Limestones, massive reddish calcilutites alternated with claystones; INI - Limestones and dolomitic limestones

and resulted in a landscape marked by the exhumed marly clayey substratum, covered at the foot of the scarps by debris settled blocks and hosting dispersed disarticulated carbonatic moving blocks. In particular, along the slab margins: double-

trenches, counter-slopes and large concave scarps characterize the sagging sector, while linear traction fractures, insulated blocks separated by open trenches and sunken collapsed area, are the dominant morphodynamic style in the right flank; in the central lowered sector, dispersed tilting – sliding rock blocks or debris slab fragments are the main landforms.

The main deep-seated phenomena are strictly connected to the presence of faults, even if in a so evolved phenomenon

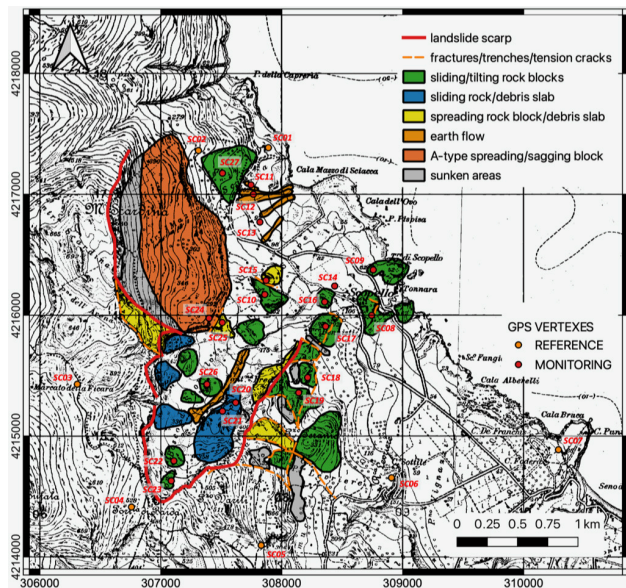


Fig. 3 - Main geomorphological features of the Scopello landslides and location of GNSS network nodes, inside (red circles) and outside (orange circles) landslides area

gravitational-driven fracturing has produced a number of retrogressive/progressive pure landslide scarps.

At the same time, while the main deep-seated dynamics evolves with very low velocities (mm/cm per year), surface gravitational processes have strongly modelled scarps and blocks (falls and toppling) and the marly clayey substratum (rotational slides and flows).

In this sense, the Scopello landslide is an example of deep to surface interaction between gravitational phenomena. In fact, the same surface rotational slides or flows phenomena, affecting the marly clayey substratum, are responsible for the lateral unlocking of the slab, resulting in the retrogressive differential settling and spreading of new blocks.

METHODOLOGICAL APPROACH

The methodological approach followed herein is based on the combination of three different surveying and monitoring technologies, to achieve a reliable structural and kinematic model of the studied DsGSD. In particular, InfraRed Thermography was employed to detect and highlight the presence of structural

alignments crossing the rock masses, along with the most relevant instability features. GPD and DInSAR were applied to survey the displacement field of the landslide, with very local wide dynamic range but discontinuous point site measurements (GNSS) and more diffused and continuous but low dynamic range spotting (DInSAR).

InfraRed Thermography

All forms of matter, owning a temperature above the absolute zero, naturally emit thermal radiation as the results of excited electron oscillations within the matter itself. Such radiation falls within the 0.1-100 μm portion of the electromagnetic spectrum, thus including parts of the ultraviolet, along with all visible and infrared regions. Nevertheless, most of the thermal radiation falls in the infrared part of the spectrum and its intensity is proportional to the temperature of the emitting material according to Stefan-Boltzmann's Law (e.g., HILLEL, 1998; SHANNON *et alii*, 2005 and references therein).

Based on this principle, the infrared radiation can be detected by specific devices, i.e. thermal cameras, which build color-scale images (thermograms) according to the surface temperature variation of the framed subjects. Such cameras operate in a range of wavelengths up to 14 μm through clear air (e.g., REES, 2001), and can be considered a reliable tool to represent, in the visible field, particular conditions that are invisible to the naked eye. The scientific casuistry involving IRT for engineering geological purposes has greatly increased in the latest years, thanks to the multiple information that it can provide on landslides (SQUARZONI *et alii*, 2008; TEZA *et alii*, 2012; CASAGLI *et alii*, 2017; FRODELLA *et alii*, 2017; PAPPALARDO *et alii*, 2018), rock mass fracturing (WU *et alii*, 2005; BARON *et alii*, 2012; MINEO *et alii*, 2015; PAPPALARDO *et alii*, 2017; PAPPALARDO & MINEO, 2019), hydraulic conductivity (PAPPALARDO, 2018), and physical properties of rocks (MINEO & PAPPALARDO, 2016; 2019).

With specific reference to rock masses, PAPPALARDO *et alii* (2021) demonstrated that the information retrievable by IRT are strongly influenced by the sun radiation, which can either enhance or hide specific features of the rock. In particular, when a rock mass is directly irradiated, information on its main morphological elements can be acquired, as hollow sectors keep lower temperatures than protruding ones. Similarly, discontinuities, sometimes filled with vegetation or earth-like material, keep lower temperatures than the bare rock. All these considerations are useful to the remote characterization of a rock mass, although their outcomes depend upon a suitable shooting position of the operator.

In this paper, thermal images were acquired in daylight conditions with the aim of achieving knowledge on both the presence of tectonic structures/particular geological conditions and instability features of the rock mass. Thermograms were

acquired by employing a high-sensitivity infrared thermal imaging camera, with a 1024 x 768 pixels infrared resolution, with a $\pm 1^\circ\text{C}$ accuracy for temperatures from 5°C to 150°C . The instrument was calibrated by setting the ambient temperature and humidity, emissivity and reflected apparent temperature. Emissivity was set to 0.93, which proved a suitable representative value for the survey of wide slope sectors where different features (such as bare rock, vegetation, talus) coexist according to literature experiences (PAPPALARDO *et alii*, 2020). The surveying spots had a frontal perspective with respect to the framed rock mass, and were located at both the southern and northern sector of the study area. Such field setting proved particularly useful for the thermal characterization of wide survey areas, where a general overview on the thermal patterns of the rock is required to highlight key elements. Observed data were validated during a post-acquisition campaign to verify the correspondence between processed images and rock mass features.

GNSS monitoring

In light of the rugged landscape, which typically characterizes the areas affected by DsGSD phenomena, as well as their remarkable areal extension, satellite monitoring result as a highly suitable geodetic monitoring system (e.g., BARBARELLA & FIANI, 1995; GILI *et alii*, 2000). In fact, in a monitoring network GNSS surveying allows for high resolution and precision measuring of large distance of baselines without imposing any inter-visibility constraints. However, considering the small amplitude of the expected deformations, monitoring network design, survey technique and scheme, number and technology of the adopted receivers are to be largely moved behind the typical using of GNSS (Global Navigation Satellite System) in classic applications (AGNESI *et alii*, 2006).

As the GNSS geodetic method measures 3D-distance between baselines, the monitoring network has to include, together with the set of monitoring vertexes, a set of reference fixed nodes. The network was designed trying to have homogeneous and short baselines, covering the range of altitudes of the entire monitored area. At the same time, a rigid coupling between the antenna of the receiver and the monitored landslide units was set, so to fit the millimetric precision we expect for normal DsGSD phenomena activity.

The Scopello GNSS monitoring network includes (Fig. 3) seven controlling vertexes (SC01, SC02, SC03, SC04, SC05, SC06 e SC07), which are located outside the known deforming landslide area, and 20 vertexes, which were coupled to the ground for monitoring slab margin (SC26 and SC27), detached isolated blocks (SC08, SC09, SC10, SC15, SC16, SC17, SC18, SC19, SC24 and SC25), large cemented debris blocks (SC14, SC20, SC21, SC22 and SC23) and marly-clay substratum (SC11, SC12 and SC13).

The results of two surveys which have been carried out in October 2004 and October 2005 by means multiple long (about 9 hours) redundant static sessions, clearly highlighted large deformations in some sectors of the Scopello landslide, caused by a relevant re-activation of the landslide, which occurred in February 2005 (AGNESI *et alii*, 2015).

Differential Interferometry SAR

Differential Interferometry SAR technique (DInSAR - FRANCESCHETTI *et alii*, 1992) has demonstrated all its capabilities in detecting displacements of the Earth's surface with subcentimetric accuracy (COLESANTI *et alii*, 2006). By the use of this technique, in fact, it is possible to obtain mean displacement rate maps, along the sensor to target distance (Line of Sight – LoS), and time series of deformations that allow to reconstruct the kinematic evolution of different natural phenomena such as landslides (PAPPALARDO *et alii*, 2018), natural and anthropic subsidence (FIASCHI *et alii*, 2017; AMMIRATI *et alii*, 2020), earthquakes (XU *et alii*, 2020) characterized by displacement rates from slow to extremely slow (HUNGR *et alii*, 2014). To the field of very slow deformations, it is possible to associate the DSGSD, which have already been studied with DInSAR technique (DI MARTIRE *et alii*, 2016; CAPPADONIA *et alii*, 2019). In this study the analysis of interferometric data for the period 2002-2018 was carried out in order to assess the kinematics of the Scopello DSGSD. The analysis was carried out in two phases:

a - interpretation of the C-band interferometric data acquired from the ENVISAT constellations, for the period 2002-2010, available within the Not-ordinary Plan of Environmental Remote Sensing (Piano Straordinario di Telerilevamento Ambientale, PST-A in Italian – COSTABILE & PACI, 2017; COSTANTINI *et alii*, 2017; DI MARTIRE *et alii*, 2017) funded by Italian Ministry of the Environment (MoE);

b - processing and interpretation of X-band data, obtained from the COSMO-SkyMed images, for the period 2016-2018, obtained within the Map-Italy Project (SACCO *et alii*, 2015) of the Italian Space Agency (ASI).

The results of this second phase were obtained using SUBSIDENCE software, developed at the Remote Sensing Laboratory (RSLab) of the Universidad Politecnica de Catalunya (Barcelona – Spain).

RESULTS

IRT

The processing of IRT images, combined with the observation of morphological features shown by the DTM of the study area (Fig. 4), returned interesting information on the presence of structural features affecting the framed slopes. Starting from the southern sector (Spot 1, Fig. 4), the first element

deserving attention is the steep slope face, exposing an evident bare surface. This element, surely visible even to the naked eye and affected by the highest surface temperature at the IR, shows an about NE-SW trend, well matching with DTM evidence (Fig. 5a). In such a field setting, in daylight condition and with sunrays directly irradiating the slope face, IRT can provide useful hint with reference to the orientation of the main exposed rock planes. In fact, planes with the same spatial orientation and dip, reasonably belonging to the same discontinuity system, will equally reflect the sunrays, thus will be affected by the same, or at least comparable, surface temperature (e.g. PAPPALARDO *et alii*, 2021 and reference therein). By constraining the range of surface temperatures within 17.4-10.7°C (Fig. 4a), so to

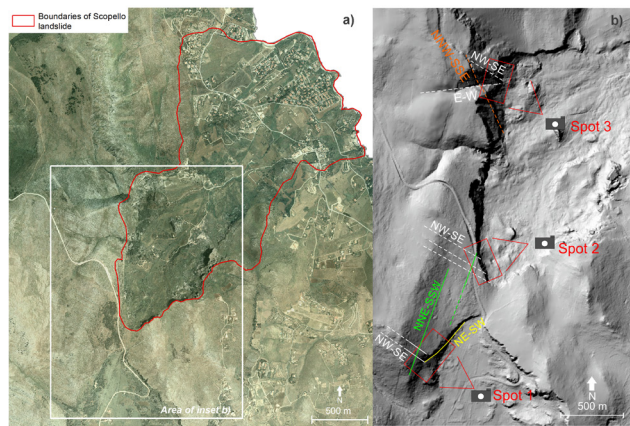


Fig. 4 - a) location of the IRT survey area in the wider frame of the Scopello landslide; b) Digital Terrain Model of the study area showing the location of thermographic shooting points and the traces of the recognized structural alignments

highlight the thermal contrast between the positive anomaly (high surface temperature) of the bare scarp and the lower temperatures of the surrounding rock mass, further positive thermal anomalies can be observed in the left side of the framed slope. These correspond to further scarps, with a ~NNE-SSW direction, well matching with a regional fault segment already known in literature. Finally, the presence of a persistent NW-SE discontinuity set, crossing the whole slope as far as its crest, is highlighted by negative anomalies (Fig. 5a).

Moving northwards (Spot 2, Fig 4), thermograms show the recurrence of linear negative anomalies (lower surface temperatures), characterized by a constant geometry (Fig. 5b-c). These correspond to discontinuity planes, shadowed at the time of the survey, extending along the whole cliff height, and producing a series of horizontal throws. Their direction matches with a NW-SE system, whose occurrence was already detected at Spot 1. In this thermogram, the presence of well-developed talus deposits at the foot of the slope testifies the predisposition of the rock mass to instability phenomena, whose occurrence is

also suggested by widespread presence of fallen blocks.

With reference to the surveying Spot 3 (Fig. 4), the thermal contrast produced in the 37.4-24.4°C surface temperature range highlights the presence of a dip-slope system exposing bare rock planes (highest temperatures) and a subvertical set represented by cold scarps. In such a setting, a relevant slope portion seems to be in a sliding kinematic asset as a wedge limited by E-W and NW-SE trending main intersecting discontinuities (Fig. 5d-e). The directions of such planes well match with the morphological

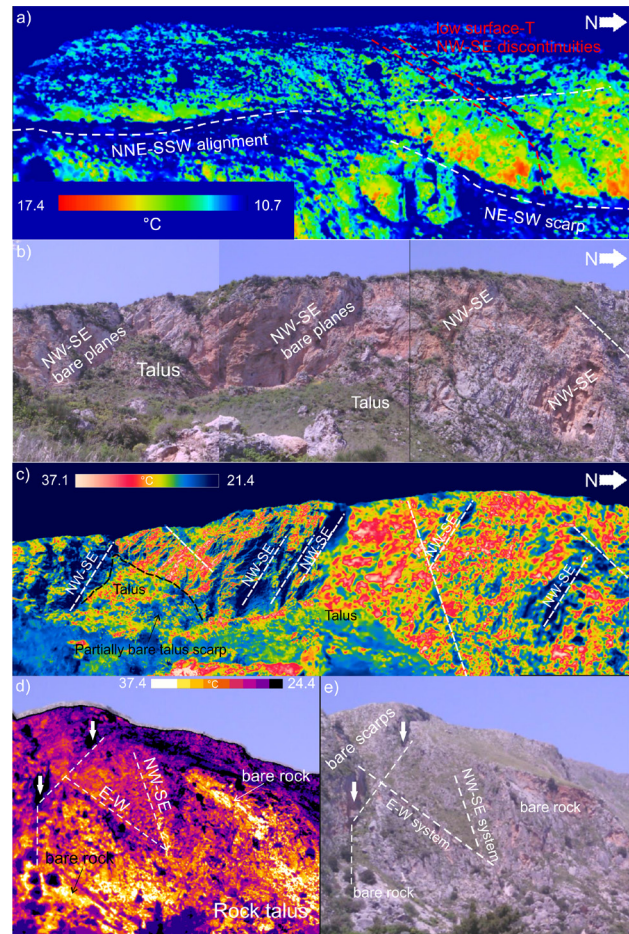


Fig. 5 - a) Thermogram acquired at Spot 1 showing the thermal contrasts between structural features and rock mass; b) slope investigated at Spot 2 with indication of the most evident discontinuities highlighted by IRT in inset c); c) surface temperature variations highlighting the NW-SE system; d) wedge sliding kinematic configuration. Arrows indicate cold areas corresponding to sub-vertical scarps; e) digital photo of the slope portion framed in inset d

setting highlighted by the DTM, with the constant occurrence of the NW-SE system suggesting its development in the study area (Fig. 3). The surveyed wedge is back-bordered by the cold subvertical scarps, probably arising from past movements of

such volume, which could be also enhanced by the presence of dip-slope planes (Fig. 5d-e). Even in this case, the presence of rock talus at the foot of the slope is index of a current evolution of the movement. Finally, the sub-vertical plane exposed at the low-temperature scarps shows an NNW-SSE direction recurring also northwards, out of the study area, but likely suggesting the regional relevance of this system.

GNSS monitoring

Data processing was performed by means of GAMIT/GLOBK v. 10.6 (HERRING *et alii*, 2015a, 2015b) in double-differences mode. The elevation cut off was set at 20° and the IGS absolute phase center variations (APCVs) for satellite and receiver antennas applied. The daily coordinates of the stations were estimated, together with the troposphere effect, in the final ionosphere free L3 solution. Using IGS final orbits, in a first step the “loose constrain” precise coordinates of the GNSS stations in the ITRF2008 frame were computed. The geodetic datum was realized by three no-net-translation conditions imposed on a set of 7 IGS08 reference stations (minimum constraint solution), which were included in the processing. The final station coordinates were obtained by constraining the fiducial GPS stations to their ITRF2008 coordinates using the Kalman filter GLOBK. The final solutions were analyzed in terms of time series of the daily solutions to check the repeatability of the coordinates as well as aggregate solutions for each survey in order to retrieve the displacement over time.

By comparing the positioning of the vertexes in October 2004 and in October 2005, 3-D displacements were derived, which clearly indicate the response of the whole landslide area to the activation in the central sector (Fig. 6). In particular, the earth/debris flows that propagated along the longitudinal axis of the area, activated at the base the movement of SC20 and SC21 debris slab units which moved northward for more than 2 m. A similar but more limited coupled response was observed in the head sector for the rock blocks at SC22 (north-northeastward) and SC23 (northward), which moved downward for some centimeters. Besides, independent displacements were observed for the lateral spreading double block system at SC18 and SC19 (north-westward, for 5-20 cm), the single block at SC14 (northward, less than 5cm) and the northernmost clayey sector at SC12 (eastward, more than 10 cm) and SC13 (north-eastward, more than 5 cm). It is worth to note that millimetric displacements were also recorded for a set of vertexes coupled to double system of disarticulated blocks: SC24-SC25, SC10-SC15, SC16-SC17.

The measured displacement resulted as very near to the resolution limit of the network, however, the spatial and morphodynamic coherence of the displacements suggest these small movements as induced by the February 2005 re-activation.

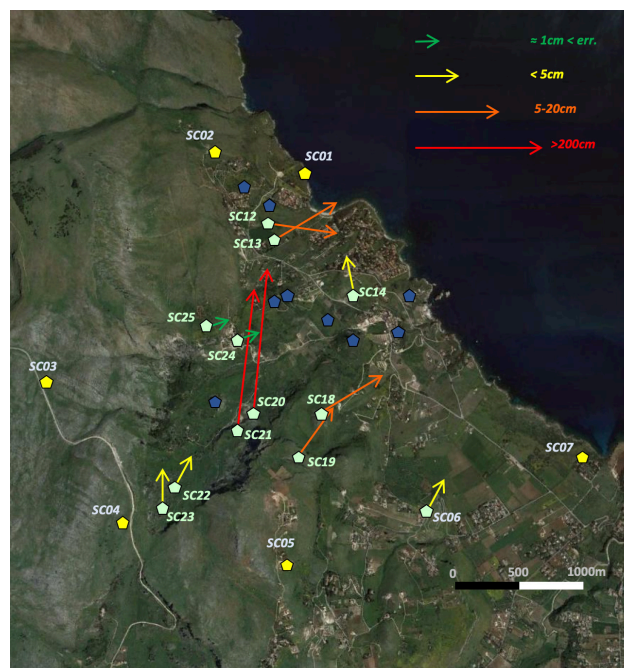


Fig. 6 - Displacement field 2004 - 2005 GNSS vertex positions. Due to the wide range of displacements, a reclassification was applied: greater than 20 cm (red arrow); between 5 and 20 cm (orange arrow); between 1 and 5 cm (yellow arrow); about 1 cm (green arrow). Vectors with modulus less 1 cm are not plotted. Blue symbols are for undisturbed vertices

DInSAR

DATA ANALYSIS FOR THE PERIOD 2002-2010

The data available on the National Geoportal (Geoportale Nazionale—GN—<http://www.pcn.minambiente.it/mattm/>) database of the MoE have allowed to implement the mean LoS displacement rate maps in the two geometries of acquisition, ascending and descending (Fig. 7). It is possible to highlight how the density and the distribution of the target was significantly different between the two geometries. As known (NOTTI *et alii*, 2010; PLANK *et alii*, 2012; CIGNA *et alii*, 2014), the visibility of targets on the ground is influenced by the acquisition geometry (incidence angle and orbit angle) and by the morphology of the investigated surface (slope and aspect).

In Fig. 7a it is possible to observe that targets with mean LoS displacement rate higher than 3 mm/year, rate considered representative of stable points (COLESANTI *et alii*, 2006), are present in different sectors of the DSGSD. In particular, the higher velocities, exceeding 0.7 cm/year were recorded on the left side and in the downstream sector. While, slightly lower rates (0.5 cm/year) in the right upstream and left downstream sector. In descending geometry (Fig. 7b), a reduced number of targets were identified and unlike what was identified in ascending geometry, the highest rates were found in the left upstream sector

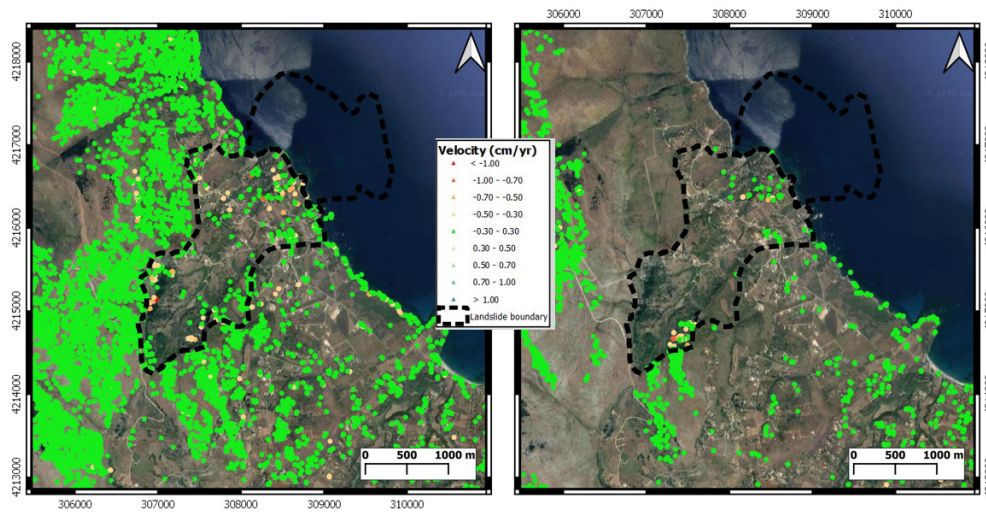


Fig. 7 - Mean displacement rate maps for ENVISAT: a) ascending; b) descending

with velocities above 0.7 cm/year. Finally, in this geometry, some targets have been identified in the downstream sector with significant rates (higher than 0.5 cm/year).

DATA ANALYSIS FOR THE PERIOD 2014-2018

In order to detect deformations, Cosmo-SkyMed images were processed by means of Differential Interferometry SAR (DInSAR) technique. Such images were obtained by means of an agreement between Department of Earth Sciences, Environment and Resources of the University of Naples Federico II and Italian Spatial Agency (ASI), in the framework of MapItaly Project.

In detail, X-band stripmap images in ascending and descending mode, characterized by a ground resolution of 3 x 3 m, acquired in the time span November 2014 and November 2018 (Tab.1) were processed using SUBSIDENCE software which implements Coherent Pixel Technique – Temporal Phase Coherence (CPT-

Satellite	Orbit	Period	# Scenes
Cosmo-SkyMed	Ascending	21/11/2014 – 16/11/2018	56
Cosmo-SkyMed	Descending	11/12/2014 – 07/11/2018	40

Tab. 1 - SAR data stacks analyzed in this study

TPC) approach (MORA *et alii*, 2003; IGLESIAS *et alii*, 2015).

CPT-TPC has been used to obtain ground displacements from satellite radar images. A detailed description of the whole algorithm can be consulted in MORA *et alii* (2003) and IGLESIAS *et alii*, 2015. The implementation of DInSAR mean displacement rate maps are obtained by seven processing steps: image co-registration, satellite orbit calculation, generation of differential interferograms, targets' selection, evaluation of linear term deformations, assessment of non-linear term rates and finally result geocoding from radar

coordinates to Universal Traverse Mercator (UTM).

In details, starting from the ascending and descending datasets, all images have been co-registered. Then, using spatial and temporal baseline thresholds of 100 m and 300 days, respectively, it was possible to identify 383 and 225 interferograms in ascending and descending orbits, respectively. In particular, the first dataset consists of 56 images acquired in ascending geometry with time-revisiting variable between 16 and 64 days in the time span November 2014 - November 2018, while the second dataset consists of 40 images acquired in descending geometry with time-revisiting variable between 16 and 96 days in the time interval December 2014 - November 2018.

CPT-TPC allows to identify points, in the investigated area, characterized by a phase quality higher than a threshold value set by the operator according to the error in the displacement estimation considered acceptable (in this case less than 1.5 mm), which in turn is a function of the expected mean displacement rate. The target selection phase is carried out by the identification of a threshold value of phase quality. Such threshold allows the selection of targets for which the error in the displacement estimate is considered acceptable (MORA *et alii*, 2003). In this case, a phase quality value equal to 0.7 has been set in both geometries in order to obtain an acceptable displacement error, lower than 1.5 mm, and to select an adequate number of points. Similarly, in this second period of analysis, it is possible to highlight a significant difference in the number of targets identified in the two acquisition geometries (Fig. 8), showing in any case a consistent growth in the density of points inside the DSGSD boundary.

While for ENVISAT data a density of about 95 and 32 targets/km² has been recorded in ascending and descending respectively, for COSMO-SKYMed the densities found are of one order of magnitude of difference, 1020 and 436 targets/km²

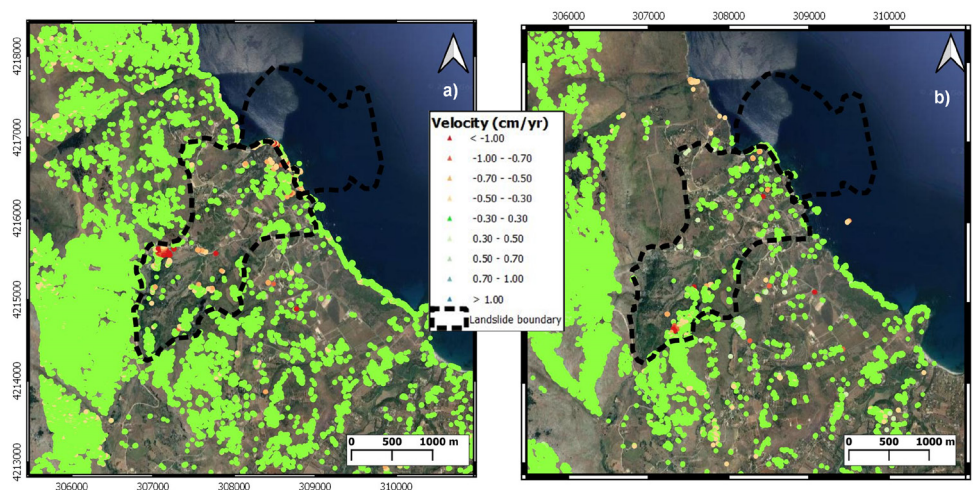


Fig. 8 - Mean displacement rate maps for COSMO-SkyMed: a) ascending; b) descending

in ascending and descending respectively.

As far as the mean displacement rates concerned, again, higher values were recorded in the upstream left sector and in the downstream central sector in both ascending and descending geometry. A further sector affected by significant rates was identified in the central portion of the DSGSD in ascending geometry.

Finally, a LoS velocity profile was plotted for some points obtained as part of the interferometric results in ascending geometry (Fig. 9). Such profile highlights the highest rates in the central sector, varying between 0.7 and 1.5 cm/year, while both upper and lower sectors the rates recorded are less than 0.3 cm/year.

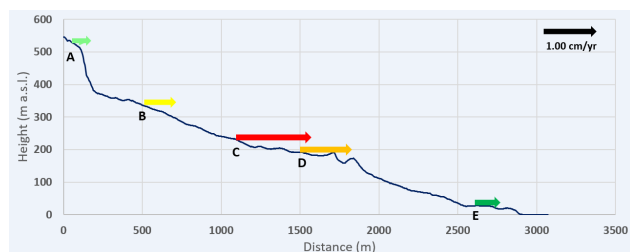


Fig. 9 - Velocity profile obtained from DInSAR ascending results

DISCUSSION AND CONCLUSIONS

The integrated analysis of the results obtained from IRT, GNSS and DInSAR surveys allows detailing and strengthening the geomorphological model of the Scopello landslide, as well as confirming the mechanisms controlling its present activity.

IRT data highlighted that the rock mass fracturing, with specific reference to the main discontinuity sets, play an important role in driving the geometry of those trenches and scarps, which

unlock the active spreading phenomena. The likely tectonic nature of most of IRT-surveyed discontinuities is suggested by a good match between data observed in the field and morphological features shown by a DTM of the area. In particular, NNE-SSW and NW-SE trending systems affect the southern sector of the Scopello landslide, where IRT highlighted the great persistence of the latter system, responsible also for crest deviations observed on the DTM (Fig. 4). To the north, this system is involved into different kinematic patterns, suggesting that the main alignments are responsible for secondary mass movements affecting the margins of the carbonate slab. As regards the monitoring component of the study, DInSAR and GNSS techniques brought to light their different complementary pros and cons. In particular, the DInSAR technique easily exploit long systematic series of recurrent satellite images where natural reflectors can be spotted and monitored, unless high peak ground accelerations do not strongly modify their relative spatial distribution. Conversely, the GNSS monitoring system, which in light of the very high costs can be more typically applied through time-discrete surveys, is robust to any ground acceleration stage with no direct resolution loss in the positioning of the vertexes. In the Scopello area, integrating DInSAR and GNSS, it has been possible to focus on the full-range kinematic of the landslide, detecting signals of very small long term deformation in a number of key sites in the central sector, with DInSAR, as well as the very large deformation induced by the earthflow in February 2005, with GNSS. Besides, in light of the coherence with the DInSAR data, small deformations close to the centimetric resolution of the GNSS survey were recovered and validated (e.g., SC24, SC25). In particular, thanks to the GNSS survey, the large deformations of February 2005 at some of the sites (Fig. 6), which are out of the dynamic range resolution of DInSAR, have been correctly detected; at the same time, the 2014-2018

DInSAR analysis captured a lasting effect at two critical sites (near SC24-SC25 and SC-20-SC21), suggesting a continuous linear deformation at the contact between rigid and ductile units deformation still active.

In light of the whole set of analysis, the Scopello landslide is to be considered as a complex/composite landslide, involving coupled shallow and deep seated deformations: on the one hand, the evolution of the deep seated deformation has produced a geomorphological setting responsible for earth flows, debris slides and rock falls/topples affecting the exhumed marly-clayey Trapanese domain substratum, the cemented talus bordering the inner margin of the carbonatic slab, the scarps produced by the spreading of the blocks, respectively. At the same time, lateral spreads, block slides, tilting and differential setting phenomena which still determine the dismantling of the overthrust slab,

are strongly accelerated by the deformation of the ductile substratum which laterally unlock the slab in the central sector.

The whole slope dynamic is strongly controlled by tectonic, which caused the rigid/ductile superimposition in the compressive stage, first, densely fracturing the whole stack in the following mainly extensional stage. The extensional deformation, together with sea level high standing phase have controlled the activation and the evolution of the phenomenon.

Deep-seated gravitational slope deformation phenomena typically result in complex landscape both in terms of morphological setting and dynamic activity. In light of the results of this research, integrating IRT, DInSAR and GNSS allows to cover a large fan of the study needs for correctly detailing the geomorphological model and interpreting the dynamic response.

REFERENCES

- AMMIRATI L., MONDILLO N., RODAS R. A., SELLERS C. & DI MARTIRE, D. (2020) - *Monitoring Land Surface Deformation Associated with Gold Artisanal Mining in the Zaruma City (Ecuador)*. *Remote Sensing*, **12** (13): 2135.
- AGLIARDI F., CROSTA G.B. & ZANCHI A. (2001) - *Structural constraints on deep-seated slope deformation kinematics*. *Eng. Geol.* **59**: 83-102.
- AGNESI V., MACALUSO T. & PIPITONE G. (1987) - *Ruolo delle deformazioni gravitative profonde di versante nell'evoluzione geomorfologica dell'area di Scopello (Trapani)*. *Boll. Soc. Geol. It.*, **106**: 231-238.
- AGNESI V., PINGUE F., ROTIGLIANO E., OBRIZZO F., DI MAGGIO C., LUZIO D. & TAMMARO U. (2006) - *Realizzazione di una rete di monitoraggio geodetico della frana di Scopello (Sicilia nord-occidentale)*. *Mem. Soc. geol. It.*, **2**: 15-27.
- AGNESI V., ROTIGLIANO E., TAMMARO U., CAPPADONIA C., CONOSCENTI C., OBRIZZO F., DI MAGGIO C., LUZIO D. & PINGUE F. (2015) - *GPS Monitoring of the Scopello (Sicily, Italy) DGSD Phenomenon: Relationships Between Surficial and Deep-Seated Morphodynamics*. In: LOLLINO G. et al. (eds) *Engineering Geology for Society and Territory*, **2**: 1321-1325. Springer, Cham.
- AGNESI V., CONOSCENTI C., DI MAGGIO C. & ROTIGLIANO E. (2017) - *Geomorphology of the Capo San Vito Peninsula (NW Sicily): An Example of Tectonically and Climatically Controlled Landscape*. In: SOLDATI M. & MARCHETTI M. (eds) *Landscapes and Landforms of Italy*, 455-465. World Geomorphological Landscapes. Springer, Cham.
- BARBARELLA M. & FIANI M. (1995) - *Controllo tramite GPS di movimenti gravitativi profondi presso La Verna*. *Mem. Soc. Geol. It.*, **50**: 34-44.
- BAROŇ I., BEČKOVSKÝ D. & MÍČA L. (2012) - *Application of infrared thermography for mapping open fractures in deep-seated rockslides and unstable cliffs*. *Landslides*, **11**: 15-27.
- CAPPADONIA C., CONFUORTO P., SEPE C. & DI MARTIRE D. (2019) - *Preliminary results of a geomorphological and DInSAR characterization of a recently identified Deep-Seated Gravitational Slope Deformation in Sicily (Southern Italy)*. *Rendiconti Online Società Geologica Italiana*, **49**: 149-156.
- CASAGLI N., FRODELLA W., MORELLI S., TOFANI V., CIAMPALINI A., INTRIERI E., RASPINI F., ROSSI G., TANTERI L. & LU P. (2017) - *Spaceborne, UAV and ground-based remote sensing techniques for landslide mapping, monitoring and early warning*. *Geoenviron. Disasters*, **4**: 9.
- CATALANO R., VALENTI V., ALBANESE C., ACCAINO F., SULLI A., TINIVELLA U., GASPARO MORTICELLI M., ZANOLLA C. & GIUSTINIANI M. (2013) - *Sicily's fold-thrust belt and slab roll-back: The SI.RI.PRO. Seismic crustal transect*. *Journal of the Geological Society*, **170** (3): 451-464.
- CATALANO R., AGATE M., BASILONE L., DI MAGGIO C., MANCUSO M. & SULLI A. (2011) - *Note illustrative della Carta Geologica d'Italia alla scala 1: 50.000, Foglio n. 593 "Castellamare del Golfo" e carta geologica allegata*. Regione Siciliana-Ispira.
- CIGNA F., BATESON L.B., JORDAN C.J. & DASHWOOD C. (2014) - *Simulating SAR geometric distortions and predicting Persistent Scatterer densities for ERS-1/2 and ENVISAT C-band SAR and InSAR applications: nationwide feasibility assessment to monitor the landmass of Great Britain with SAR imagery*. *Remote Sens. Environ.*, **152**: 441-466.
- COLESANTI C. & WASOWSKI, J. (2006) - *Investigating landslides with space-borne synthetic aperture radar (SAR) interferometry*. *Eng. Geol.*, **88** (3-4): 173-199.
- COSTANTINI M., FERRETTI A., MINATI F., FALCO S., TRILLO F., COLOMBO D., NOVALI F., MALVAROSA F., MAMMONE C., VECCHIOLI F., RUCCI A., FUMAGALLI A., ALLIEVI J., CIMINELLI M.G. & COSTABILE S. (2017) - *Analysis of surface deformations over the whole Italian territory by interferometric processing of ERS, Envisat and COSMO SkyMed radar data*. *Remote Sens. Environ.*, **202**: 250-275.

- CROSTA G.B. (1996) - *Landslide, spreading, deep seated gravitational deformation: analysis, examples, problems and proposals*. *Geografia Fisica e Dinamica Quaternaria*, **19**: 297-313.
- DEVOTO S., MACOVAZ V., MANTOVANI M., SOLDATI M. & FURLANI S. (2020) - *Advantages of Using UAV Digital Photogrammetry in the Study of Slow-Moving Coastal Landslides*. *Remote Sens.*, **12**: 3566.
- DI MAGGIO C., MADONIA G. & VATTANO M. (2014) - *Deep-seated gravitational slope deformations in western Sicily: Controlling factors, triggering mechanisms, and morpho-evolutionary models*. *Geomorphology*, **208**: 173-189.
- DI MAGGIO C., MADONIA G., VATTANO M., AGNESI V. & MONTELEONE S. (2017) - *Geomorphological evolution of western Sicily, Italy*. *Geologica Carpathica*, **68**: 80-93.
- DI MARTIRE D., NOVELLINO A., RAMONDINI M. & CALCATERRA D. (2016) - *A-Differential Synthetic Aperture Radar Interferometry analysis of a Deep-Seated Gravitational Slope Deformation occurring at Bisaccia (Italy)*. *Science of The Total Environment*, **550**: 556-573.
- DI MARTIRE D., PACI M., CONFUORTO P., COSTABILE S., GUASTAFERRO F., VERTA A. & CALCATERRA D. (2017) - *A nation-wide system for landslide mapping and risk management in Italy: The second Not-ordinary Plan of Environmental Remote Sensing*. *International Journal of Applied Earth Observation and Geoinformation*, **63**: 143-157.
- DRAMIS F. & SORRISO-VALVO M. (1994). *Deep-seated gravitational slope deformations, related landslides and tectonics*. *Eng. Geol.*, **38**: 231-243.
- FIASCHI S., TESSITORE S., BONÌ R., DI MARTIRE D., ACHILLI V., BORGSTROM S., IBRAHIM A., FLORIS M., MEISINA C., RAMONDINI M. & CALCATERRA D. (2017) - *From ERS-1/2 to Sentinel-1: two decades of subsidence monitored through A-DInSAR techniques in the Ravenna area (Italy)*. *GIScience & Remote Sensing*, **54** (3): 305-328.
- FIORUCCI M., MARMONI G.M., MARTINO S. & MAZZANTI, P. (2018) - *Thermal Response of Jointed Rock Masses Inferred from Infrared Thermographic Surveying (Acuto Test-Site, Italy)*. *Sensors* **18**: 2221.
- FRANCESCHETTI G., MIGLIACCIO M., RICCIO D. & SCHIRINZI G. (1992) - *SARAS: a synthetic aperture radar (SAR) raw signal simulator*. *IEEE Trans. Geosci. Remote Sens.*, **30**: 110-123.
- FRODELLA W., ELASHVILI M., SPIZZICHINO D., GIGLI G., ADIKASHVILI L., VACHEISHVILI N., KIRKITADZE G., NADARAIA A., MARGOTTINI C. & CASAGLI N. (2020) - *Combining infrared thermography and UAV digital photogrammetry for the protection and conservation of rupestrian cultural heritage sites in Georgia: A methodological application*. *Remote Sensing*, **12**: 5.
- FRODELLA W., GIGLI G., MORELLI S., LOMBARDI L. & CASAGLI N. (2017) - *Landslide Mapping and Characterization through Infrared Thermography (IRT): Suggestions for a Methodological Approach from Some Case Studies*. *Remote Sens.*, **9**: 1281.
- GILI J.A., COROMINAS J. & RIUS J. (2000) - *Using Global Positioning System techniques in landslide monitoring*. *Engineering Geology*, **55**: 167-192.
- HERRING T.A., KING R.W., FLOYD M.A. & MCCLUSKY S.C. (2015a) - *GAMIT Reference Manual: GPS Analysis at MIT, Release 10.6*. Department of Earth, Atmospheric and Planetary Sciences, Massachusetts Institute of Technology, Cambridge MA.
- HERRING T.A., FLOYD M.A., KING R.W. & MCCLUSKY S.C. (2015b) - *GLOBK Reference Manual: Global Kalman Filter VLBI and GPS analysis program, Release 10.6*. Department of Earth, Atmospheric and Planetary Sciences, Massachusetts Institute of Technology, Cambridge MA.
- HILLEL D. (1998) - *Environmental Soil Physics 771*. New York: Academic Press.
- HUNGR O., LEROUÉIL S. & PICARELLI L. (2014) - *The Varnes classification of landslide types, an update*. *Landslides*, **11** (2): 167-194.
- IGLESIAS R., MONELLS D., LÓPEZ-MARTÍNEZ C., MALLORQUÍ J.J., FABREGAS X. & AGUASCA A. (2015). *Polarimetric optimization of Temporal Sublook Coherence for DInSAR applications*. *IEEE Geosci. Remote Sens. Lett.*, **12** (1): 87-91.
- MINEO S. & PAPPALARDO G. (2019) - *InfraRed Thermography presented as an innovative and non-destructive solution to quantify rock porosity in laboratory*. *International Journal of Rock Mechanics and Mining Sciences*, **115**: 99-110.
- MINEO S. & PAPPALARDO G. (2016) - *Preliminary results on the estimation of porosity in intact rock through InfraRed Thermography*. *Rend. Online Soc. Geol. It.*, **41**: 317-320.
- MINEO S., CALCATERRA D., PERRIELLO ZAMPELLI S. & PAPPALARDO G. (2015) - *Application of Infrared Thermography for the survey of intensely jointed rock slopes*. *Rend. Online Soc. Geol. It.*, **35**: 212-215.
- MORA O., MALLORQUÍ J.J. & BROQUETAS A. (2003) - *Linear and nonlinear terrain deformation maps from a reduced set of interferometric sar images*. *IEEE Transactions on Geoscience and Remote Sensing*, **41**: 2243-2253.
- NOTTI D., DAVALILLO J.D., HERRERA G. & MORA O. (2010) - *Assessment of the performance of Xband satellite radar data for landslide mapping and monitoring: Upper Tena Valley case study*. *Nat. Hazards Earth Syst. Sci.*, **10**: 1865-1875.
- PAPPALARDO G. (2018) - *First results of infrared thermography applied to the evaluation of hydraulic conductivity in rock masses*. *Hydrogeol J.*, **26** (2): 417-428.
- PAPPALARDO G. & MINEO S. (2019) - *Study of Jointed and Weathered Rock Slopes Through the Innovative Approach of InfraRed Thermography*. In: PRADHAN S., VISHAL V. & SINGH T. (2019 EDS) *Landslides: Theory, Practice and Modelling*. *Advances in Natural and Technological Hazards Research*, vol **50**. Springer, Cham..

- PAPPALARDO G., MINEO S., CARBONE S., MONACO C., CATALANO D. & SIGNORELLO G. (2021) - *Preliminary recognition of geohazards at the natural reserve "Lachea Islet and Cyclop Rocks" (Southern Italy)*. Sustainability, **13**: 1082.
- PAPPALARDO G., MINEO S., IMPOSA S., GRASSI S., LEOTTA A., LA ROSA F. & SALERNO D. (2020) - *A quick combined approach for the characterization of a cliff during a post-rockfall emergency*. Landslides, **17**: 1063-1081.
- PAPPALARDO G., MINEO S., ANGRISANI A.C., DI MARTIRE D. & CALCATERRA D. (2018) - *Combining field data with infrared thermography and DInSAR surveys to evaluate the activity of landslides: the case study of Randazzo Landslide (NE Sicily)*. Landslides, **15**: 2173-2193.
- PAPPALARDO G., MINEO S. & CALCATERRA D. (2017) - *Geomechanical Analysis Of Unstable Rock Wedges By Means Of Geostructural And Infrared Thermography Surveys*. Italian Journal of Engineering Geology and Environment, Special Issue (2017), 93-101.
- PASUTO A. & SOLDATI M. (2013) - *Lateral spreading*. Treatise on geomorphology, 239-248.
- PLANK S., SINGER J., MINET C. & THURO K. (2012) - *Pre-survey suitability evaluation of the differential synthetic aperture radar interferometry method for landslide monitoring*. Int. J. Remote Sens., **33** (20): 6623-6637.
- REES W.G. (2001) - *Physical principles of remote sensing*. Cambridge University Press, 343.
- SACCO P., BATTAGLIERE M.L., DARAIO M.G. & COLETTA A. (2015) - *The COSMO-SkyMed constellation monitoring of the Italian territory: Map Italy project*. In Proc. of 66th International Astronautical Congress (IAC 2015), 12-16.
- SAVAGE W.Z. & VARNES D.J. (1987) - *Mechanism of gravitational spreading of steep-sided ridges («sackung»)*. Bull. Int. Assoc. Eng. Geol., **35**: 31-36.
- SHANNON H.R., SIGDA J.M., VAN DAM R.L., HANDRICKX J.M.H. & MCLEMORE V.T. (2005) - *Thermal camera imaging of rock piles at the Questa Molybdenum Mine, Questa, New Mexico*. Proc. 2005 National Meeting of the American Society of Mining and Reclamation, June 19–23, 2005, ASMR, 1015–1028.
- SQUARZONI C., GALGARO A., TEZA G., ACOSTA C.A.T., PERNITO M.A. & BUCCERI N. (2008) - *Terrestrial laser scanner and infrared thermography in rock fall prone slope analysis*. Geophysical Research Abstracts **10**, EGU2008-A-09254, EGU General Assembly 2008.
- TEZA G., MARCATO G., CASTELLI E. & GALGARO A. (2012) - *IRTROCK: A MATLAB toolbox for contactless recognition of surface and shallow weakness of a rock cliff by infrared thermography*. Computers & Geosciences, **45**: 109-118.
- VARNES D.J., RADBRUCH HALL D. & SAVAGE W.Z. (1989) - *Topographic and structural conditions in areas of gravitational spreading of ridges in the Western United States*. US Geological Survey, Professional Papers **1496**: 1-28.
- WU J.H., LIN H.M., LEE D.H. & FANG S.C. (2005) - *Integrity assessment of rock mass behind the shotcreted slope using thermography*. Engineering Geology, **80**: 164-173.
- XU X., SANDWELL D.T. & SMITH-KONTER B. (2020) - *Coseismic displacements and surface fractures from Sentinel-1 InSAR: 2019 Ridgecrest earthquakes*. Seismological Research Letters, **91** (4): 1979-1985.

Received March 2021 - Accepted April 2021